Environmental Pollution 266 (2020) 115290

Contents lists available at ScienceDirect

Environmental Pollution

journal homepage: www.elsevier.com/locate/envpol

# Imidacloprid disturbed the gut barrier function and interfered with bile acids metabolism in mice☆

Guiling Yang [a], Xianling Yuan [b], Cuiyuan Jin [b], Dou Wang [a], Yanhua Wang [a, **], Wenyu Miao [b], Yuanxiang Jin [b, *]

[a] State Key Laboratory for Quality and Safety of Agro-products, Key Laboratory for Pesticide Residue Detection of Ministry of Agriculture, Laboratory (Hangzhou) for Risk Assessment of Agricultural Products of Ministry of Agriculture, Institute of Quality and Standard for Agro-products, Zhejiang Academy of Agricultural Sciences, Hangzhou, 310021, Zhejiang, China
[b] College of Biotechnology and Bioengineering, Zhejiang University of Technology, Hangzhou, 310032, Zhejiang, China

ARTICLE INFO

*Article history:*
Received 25 May 2020
Received in revised form
2 July 2020
Accepted 19 July 2020
Available online 8 August 2020

*Keywords:*
Imidacloprid
Liver injury
Bile acids
Gut barrier
Gut microbiota

ABSTRACT

The toxicity of neonicotinoid insecticide imidacloprid (IMI) to mammals has recently received increasing attention. However, the effects of IMI on the gut barrier and liver function of male C57BL/6J mice are still unknown. The study showed that exposure to IMI could reduce relative liver weights, change hepatic tissue morphology and induce hepatic oxidative stress. The gut barrier function was greatly impaired by IMI exposure, which might increase the body's susceptibility to harmful substances in the gut. Meanwhile, the synthesis and metabolism of hepatic bile acids (BAs) was also affected by IMI exposure. The levels of serum and hepatic total bile acids (TBAs) decreased; in contrast, the fecal TBA levels increased after exposure to 30 mg/L IMI for 10 weeks. Sequencing of colonic contents revealed that the operational taxonomic units (OTUs) and α-diversity index increased and that the gram-negative bacteria overgrew, indicating that the balance of the gut microbiota was disrupted. The present study indicated that subchronic exposure to IMI interfered with the gut barrier function, interfering with BAs metabolism and causing gut microbiota imbalance in male C57BL/6J mice. Taken together, IMI residues appear to be potentially toxic to mammals and even humans.



## 1. Introduction

Pesticide residues pose a potential toxic threat to nontarget animals or even humans (Damalas and Eleftherohorinos, 2011; Yuan et al., 2019). A number of previous studies have exposed the toxicity of pesticides to mice on the liver (Wu et al., 2018a), kidney (Wei et al., 2014), nervous system (Zhang et al., 2019a), immune system (Banerjee, 1999) and endocrine system (Jin et al., 2019a).

*Abbreviations:* CA, Cholic Acid; LCA, Lithocholic Acid; DCA, Deoxycholic Acid; UDCA, Ursodeoxycholic Acid; CDCA, Chenodeoxycholic Acid; TCA, Taurocholic Acid; GCA, Glycocholic Acid; TLCA, Taurolithocholate Acid; GLCA, Glycolithocholic Acid; TDCA, Taurodeoxycholate Acid; TUDCA, Tauroursodeoxycholate Acid; TCDCA, Taurochenodeoxycholate Acid; GDCA, Glycodeoxycholate Acid; GCDCA, Glycochenodeoxycholate Acid; GUDCA, Glycoursodeoxycholic Acid; ALT, alanine aminotransferase; AST, aspartate aminotransferase; ALP, alkaline phosphatase; Sod1, superoxide dismutase 1; Cat, catalase; Gpx1, glutathione peroxidase 1; Gpx2, glutathione peroxidase 2; Gsta1, glutathione-S-transferase A1; Gss, glutathione synthetase; Gr, glutathione reductase; Ho-1, heme oxygenase 1; Cyp7a1, cholesterol 7a-hydroxylase; Cyp8b1, sterol 12α-hydroxylase; Cyp27a1, sterol 27-hydroxylase; Cyp7b1, oxysterol 7α-hydroxylase; Slc27a5, solute carrier family 27 member 5; Baat, bile acid CoA, amino acid N-acyltransferase; Bsep, bile salt export pump; Mrp2, multi drug resistance associated protein 2; Mrp3, multi drug resistance associated protein 3; Ntcp, Na + taurocholate cotransporting peptide; Fxr, farnesoid X receptor; Shp, small heterodimer partner; Asbt, the apical sodium-dependent bile acid transporter; Ostα, Organic solute transporters α; Ostβ, organic solute transporters β; I-babp, ileal bile acid binding protein; Fgf15, fibroblast growth factor 15; Muc1, mucin 1; Muc2, mucin 2; Muc3, mucin 3; Klf4, kruppel-like factor 4; Defa3, alpha-defensin 3; Defa20, alpha-defensin 20; Pla2g4a, phospholipase A2, Group IIA; Mmp-7, matrix metalloproteinase-7; Amg4, amtolmetin guacyl 4; Reg3, regenerating gene; Lyz, lysozyme; Ano1, anoctamin 1; Nkcc1, Na-K-2Cl cotransporter 1; Cftr, cystic fibrosis transmembrane conductance regulator; Slc26A3, solute carrier family 26 member 3; Slc26A6, solute carrier family 26 member 6; Nhe3, sodium-hydrogen exchanger 3; Zo-1, zonula occludens-1.

☆ This paper has been recommended for acceptance by Christian Sonne.

* Corresponding author.
** Corresponding author.
*E-mail addresses:* wangyanh79@hotmail.com (Y. Wang), jinyx@zjut.edu.cn (Y. Jin).

https://doi.org/10.1016/j.envpol.2020.115290
0269-7491/

Imidacloprid (IMI), as a first-generation neonicotinoid insecticide, has a much higher affinity for nicotinic acetylcholine receptor (nAChR) in insects than that in mammals (Sun et al., 2016; Daisley et al., 2017). However, several studies reported that IMI could be metabolized by mammals and then converted into more toxic metabolites, for example, desnitro metabolite (DN-IMI) and nitromethylene analogue (CH-IMI) (Brunet et al., 2004), indicating that the mammalian toxicity of IMI could not be ignored. An investigation identified four cases of liver injury among 128 cases of IMI ingestion patients from 2010 to 2016 in Thailand (Sriapha et al., 2020). What's more, 15 mg/kg/day IMI can decrease the body weight of male albino mice, caused a significant elevation of serum clinical chemistry parameters including AST, ALT, AKP and total bilirubin (TBIL) (Arfat et al., 2014).

Enterohepatic circulation is vital for maintaining the health of the body (Fader et al., 2017). The gut directly contacts food. There is an efficient multifaceted gut barrier system with physical (structural and functional intestinal epithelial cells and tight junction-associated proteins), chemical [mucus, antibacterial peptides (AMPs) and bile acids (BAs)], immunological (Peyer's patches, M cells and submucosal lymphoid tissue) and microbial (normal commensal bacteria's colonization resistance to pathogenic bacteria) components that prevents the entry of most pathogens (Dupont et al., 2014; Mukherjee and Hooper, 2015; Mu et al., 2017). The destruction of the intestinal barrier will make the body more susceptible to exogenous poisons, further leading to metabolic disorders, including impaired BA metabolism. In addition, intestinal BAs can inhibit excessive proliferation and displacement of the gut microbiota and have a certain effect on maintaining the balance of the gut microbiota and stabilizing intestinal barrier function (Rizzetto et al., 2018; Ferrell and Chiang, 2019). Polystyrene microplastics remain in the intestines of mice, reducing the secretion of intestinal mucus and impairing intestinal barrier function, and can cause disorders of BAs metabolism (Jin et al., 2019b). Chronic exposure to low doses of pesticide imazalil can induce liver damage, disorders of bile acid metabolism and disturbed the intestinal barrier function of the mice (Jin et al., 2018a, 2018b). Generally, changes in serum BAs levels are tightly associated with hepatobiliary diseases (Ferrell and Chiang, 2019). Therefore, it is necessary to measure the effect of IMI on the synthesis, transport and function of BAs in mice.

Residues of IMI can enter the soil, water and air and ultimately harm nontarget animals, including humans. According to previous research, 3.8–96.8 ng/L IMI was detected in surface water samples from Forester Creek, a tributary to the San Diego River (Batikian et al., 2019). A chronic dietary reference dose for IMI based on the no-observed-adverse-effect level to be 0.057 mg $kg^{-1}$ $d^{-1}$ has enacted by the U.S. Environmental Protection Agency (Zhang et al., 2019b). One survey found that the estimated intake of neonicotinoid insecticides was 710.38 ng $kg^{-1}$ bodyweight (bw) $d^{-1}$ in China, of which IMI was the most frequently detected (Chen et al., 2019). How IMI impacts the gut barrier, gut microbiota, BAs metabolism and liver function in mammals is unclear. The mice, especially for C57BL/6J, used as the test animal, because it is one of the representatives of typical mammals. Here, the toxic effects of IMI to mice on the intestinal barrier, gut microbiota, and liver were elucidated. We hoped that the current experiment could contribute to the correct assessment of the toxicity of IMI.

## 2. Materials and methods

### 2.1. Materials

Commercial imidacloprid (CAS: 138261-41-3, purity: ≥98%) was obtained from YuanYe Company (Shanghai, China). Phosphate-buffered saline (PBS, 20x, pH 7.4, Sangon Biotech, E607016). Methanol and acetonitrile were purchased from Sigma-Aldrich (≥99.9%, St Louis, Missouri).

### 2.2. Animals study

6 week of age male C57BL/6J mice were provided by the China National Laboratory Animal Resource Center (Shanghai, China) and were fed a standard chow diet. They were maintained at 24 ± 1 °C with a cycle of 12 h light and dark. Thirty-two mice were equally and randomly divided into four groups (n = 8), one control group and three exposure groups. The control group was administered deionized water. Three groups were orally respective exposed to IMI (3, 10 or 30 mg/L) by drinking water for 70 days, respectively. Each mouse in four groups consumed about an average of 0, 0.5, 1.67, 5 mg $kg^{-1}$ bw $d^{-1}$ IMI. One survey founded that 5 and 10 mg $kg^{-1}$ bw $d^{-1}$ IMI is no observed adverse effect level (NOAEL) for mice (Arfat et al., 2014). In this study, the dosages were set under the NOAEL. Water and food were available ad libitum during the exposure. Fecal pellets were regularly collected at 8 a.m. every week and stored at −40 °C for further use.

Mice were fasted for at least 12 h before sacrifice and were euthanized by ether. Samples including serum, liver, ileum, colon and colonic contents were collected as quickly as possible, followed by storage at −80 °C. For histopathological analysis, a piece of liver or colon were fixed in 0.1% (w/v) paraformaldehyde immediately. All experimental procedures were carried out according to ethical guidelines and regulations approved by the Zhejiang University of Technology.

### 2.3. Determination of the TBAs in the serum, liver and feces

The total bile acids (TBAs) in the serum, liver and feces were quantified by the commercial kits (Nanjing Jiancheng Bioengineering Institute, Nanjing, China). To analyze the hepatic and fecal TBAs, all samples were homogenized in nine times the volume (v/w) of PBS. After centrifuging the homogenate at 3000 rpm for 10 min, the supernatant was taken for experiment. Protein concentrations in the liver and feces were determined by the bicinchoninic acid (BCA) protein kit (Beyotime Institute of Biotechnology, Shanghai, China).

### 2.4. Profiling of BAs in the plasma

A total of 100 μL of serum samples from 5 mice, randomly selected from the control group and the 30 mg/L IMI treatment group, were added to 300 μL of distilled water containing internal standards (1/1). The mixture was centrifuged at 4 °C and 11,000 rpm for 5 min. After centrifugation, 300 μL of the supernatant was moved to microcentrifuge tubes for lyophilization and reconstitution with 100 μL of acetonitrile/methanol (25/8). Then, the samples were centrifuged by 11,000 rpm for 5 min at 4 °C, and 80 μL of supernatant was used for UPLC-MS/MS analysis (ACQUITY UPLC I-Class/Xevo TQD IVD, Water Corp., Milford, MA, USA).

### 2.5. Alterations of Zo-1 in the colon and Cyp7a1, AST, ALT, ALP in the liver

The colon and liver were homogenized with nine volumes (v/w) of precooled PBS to acquire the supernatant (3000×*g*, 4 °C, 10 min). These supernatants are used to determine the content of colonic Zo-1 and hepatic Cyp7a1 using commercial enzyme-linked ELISA kits (Shanghai Enzyme-linked Biotechnology, China). Hepatic AST, ALT and ALP levels were analyzed by kits form the Nanjing Jiancheng Institute of Biotechnology (Najing, China). As mentioned

above in section 2.3, the concentration of protein in each sample was determined correspondingly.

### 2.6. Histopathological examination

Small pieces of liver or colon were collected and fixed in 0.1% (w/v) paraformaldehyde immediately. The fixed tissues were embedded in paraffin wax at 56 °C. Then, 5 μm-thick hepatic and colonic sections are respectively stained with hematoxylin & eosin (H&E) and alcian blue-periodic acid Schiff (AB-PAS) for histochemical analysis. Refer to this article for the calculation of the number of cell nucleus (Sheng et al., 2018).

### 2.7. Immunohistochemical analysis

Dewaxed in xylene, the colonic paraffin sections were recovered by heating in EDTA antigen retrieval buffer (pH 9.0) and incubated with a peroxidase-blocking solution to block endogenous peroxidases (Yuan et al., 2020) After antigen retrieval was performed, polyclonal anti-Muc1 (A00187, Boster Biological Technology, Ltd., Wuhan, China) antibody at a dilution of 1:200 was applied overnight in a wet box. Next, HRP-conjugated secondary antibodies were added to the slices, and incubation for 50 min at 25 °C, stained with diaminobenzidine, and counterstained with hematoxylin.

### 2.8. Quantitative real-time PCR analysis

The Biozol reagent (Takara Biochemicals, China) was used to isolate the total RNA from tissues. Then a reverse transcriptase kit (Vazyme, China) was used to synthesize cDNA. RT-qPCR was carried out using SYBR Green (Vazyme, China) and qTOWER3G platform (Analytik Jena AG, Germany). Primer sequences of genes related to oxidative stress, BA metabolism, gut barrier in mice were used according to previous reports (Fader et al., 2017; Csanaky et al., 2018; Pan et al., 2019; Luo et al., 2019; Liang et al., 2019; Wu et al., 2018b). 18S RNA served as an endogenous control. The cycling procedure were configured as following: 1 min at 95 °C; 15 s at 95 °C (40 cycles); 60 s at 60 °C. The quantification of gene expression in IMI-treated groups was calculated with controls set as 100% (Xia et al., 2018).

### 2.9. Fecal bacterial DNA analysis

Total genomic bacterial DNA was extracted from fecal samples and qPCR amplification in the present study were performed as methods described previously (Jin et al., 2018b).

### 2.10. Illumina MiSeq sequencing

Briefly, the bacteria were extracted from the colonic contents (n = 5). After quality inspection, the universal primers F319/R806 were used to amplify the 16S rRNA genes (V3-V4 regions). The purified PCR products pooled on the Illumina MiSeq platform followed by QIIME (version 1.6.0) to analysis the variation of experimental results (Pan et al., 2019).

### 2.11. Data analysis

All the values were showed as the mean ± SEM. Image pro-Plus 6.0, GraphPad Prism 7.0, Photoshop, Microsoft PowerPoint were used to analyze and draw pictures. One-way analysis of variance (ANOVA) and Dunnett's protected least significant difference tests were used to evaluate the differences among each group using SPSS 24.0 (SPSS, Chicago, Illinois). $p < 0.05$ was indicated as significant difference.

## 3. Results

### 3.1. IMI exposure induced hepatic toxicity

Compared with the control, the relative liver weights of the three IMI-treated groups decreased significantly (Fig. 1A). In addition, the H&E staining showed histopathological evidence of IMI-induced toxic effects on livers (Fig. 1B). The relative number of nuclei compared with the control within defined liver slice areas was significant decrease (Fig. 1C). Moreover, corresponding to the histopathological changes found in the liver slices, 30 mg/L IMI exposure elevated the AST and ALP activities in the serum (Fig. 1D).

### 3.2. The transcription of oxidative stress related genes in the liver

IMI exposure influenced the mRNA levels of oxidative stress related genes (Fig. 1E). Upregulation of *Gsta1*, *Gpx2*, *HO-1* and *Cat* transcription was observed in the 30 mg/L IMI-treated groups. In contrast, the mRNA levels of *Gpx1* decreased significantly in the mouse livers exposed to 30 mg/L IMI for 70 days. However, transcriptions of *Sod1*, *Gss* and *Gr* in the liver were unaffected by IMI exposure.

### 3.3. IMI exposure altered BA profiles

In the 30 mg/L IMI-treated for 70 days group, the serum and hepatic TBA levels significantly decreased, whereas the fecal TBAs increased (Fig. S1).

Considering that TBA levels significantly changed only in the 30 mg/L IMI-treated group, we further studied the BA profiling of plasma samples in the 30 mg/L IMI-treated groups and vehicle control. The results showed that the levels of 9 of the detected BAs changed significantly in mice after 70 days of IMI exposure (Fig. 2A and B). The ratio of conjugated/unconjugated BAs was increased (Fig. 2C); however, the ratio between primary and secondary BAs was not significantly affected (Fig. 2D). By building a PLS-DA model (Fig. 2E), we screened five types of BAs with variable importance in projection (VIP) values > 1.0, namely, CA, CDCA, LCA, DCA, and ursodeoxycholic acid (UDCA), and the levels of all of them decreased in the 30 mg/L IMI-treated group (Fig. 2A and B).

### 3.4. IMI exposure altered BAs metabolism

Compared with the vehicle control, the protein levels of hepatic Cyp7a1 decreased significantly in the 30 mg/L IMI-treated group (Fig. 3A). BA metabolism-related genes were also changed after IMI exposure at the transcriptional level. For example, IMI exposure decreased the mRNA of *Cyp7a1*, *Slc27a5*, the sterol 12-hydroxylase *Cyp8b1,* and *Baat*. The mRNA levels of hepatic *Cyp27a1* and *Cyp7b1* were not affected by IMI exposure (Fig. 3B). In addition, exposure to 30 mg/L IMI decreased the mRNA levels of *Mrp2* and *Mrp3* but increased the mRNA of t *Ntcp* (Fig. 3C). We also quantified the mRNA levels of the transcription factors regulating BA synthesis. The hepatic mRNA of the major BA "sensor" *Fxr* and the Fxr transcriptional target gene *Shp* were not affected (Fig. 3D).

In the ileum, IMI exposure decreased the mRNA levels of the luminal transporter *Asbt*. The levels of *Ostα* and *Ostβ*, known as basolateral transporters, decreased in the ileum of mice when exposed to 30 mg/L (Fig. 3E). Interestingly, exposure to IMI decreased the mRNA levels of *Fxr* and *Fgf15*, which are the main

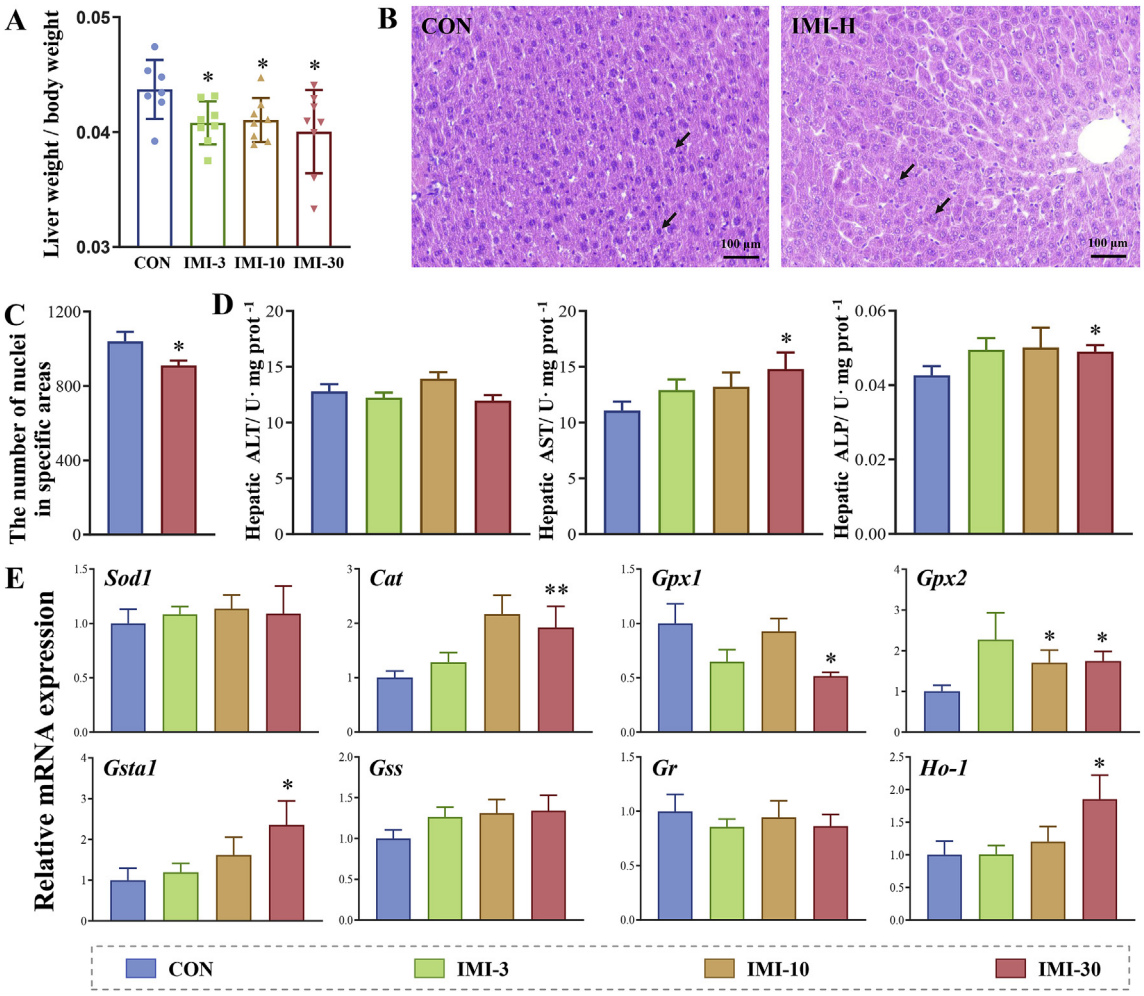


**Fig. 1.** Effects of oral IMI exposure on liver function in mice. The relative liver weights (A); histopathological analysis of liver sections stained with hematoxylin and eosin (H&E; 100 ×). Black arrow indicates cell nuclei (B); the average number of cell nuclei within a defined area acquired by manual counting (C); the activities of AST, ALT and ALP in the liver (D); the mRNA levels of genes related to oxidative stress (E). All the data are expressed as the means ± SEMs. An asterisk indicates a significant difference (*at $p < 0.05$; **at $p < 0.01$) between the control and IMI-treated groups.

regulators of BA homeostasis in the ileum (Fig. 3F).

### 3.5. Effects of IMI exposure on the gut barrier in the colon

AB-PAS staining showed that the secretion of mucus increased significantly in the colon of mice after exposure to 30 mg/L IMI (Fig. 4A). The quantification of the mucus coverage ratio further comformed the increases in mucus secretion (Fig. 4B). In addition, immunohistochemical staining of Muc-1 in the colon showing that the protein levels of colonic Muc1 from the 30 mg/L IMI-treated group were much higher than the control (Fig. 4 C and D). 30 mg/L IMI exposure for 70 days downregulated the expression levels of mucus secretion-related genes in the colon, except for increasing the expression of *Muc-1* (Fig. 4E). The transcriptional levels of AMP secretion-related genes, including *Defa3*, *Defa20*, *Lyz* and *Mmp-7*, were also downregulated in the 30 mg/L IMI-treated mice (Fig. 4F). After exposure to 30 mg/L IMI for 70 days, the mRNA levels of *Ano1*, *Slc26A3* and other ion transport-related genes in the mouse colon has decreased (Fig. 4G). The mRNA levels of *Zo-1* and *Claudin-1* were also significantly downregulated in the colon (Fig. 4H). Moreover, the protein level of Zo-1 also decreased in the high-dose IMI group (Fig. 4I). More importantly, the serum lipopolysaccharide (LPS) content had an upward trend, but it was not statistically significant (Fig. 4J).

### 3.6. Effects of IMI-derived colonic gut microbial dysbiosis

We next analyzed the main constituents of the fecal microbiota at the phylum level. As shown in Fig. 5A, the relative abundance of *β-proteobacteria*, *γ-proteobacteria* and *Verrucomicrobia* in the 30 mg/L IMI-treated group increased significantly when compared with the control. Therefore, the microbiomes in the colonic contents of the control and high-dose groups were analyzed by using 16S RNA gene sequencing. A total of 520 operational taxonomic units (OTUs) were found in the two sequencing groups (Fig. 5B). In addition, 52 and 208 OTUs were detected only in the control and 30 mg/L IMI-treated groups, respectively (Fig. 5B). Moreover, based on α-diversity, the Chao index of mice showed an upward trend (Fig. 5C). Principal coordinate analysis (PCoA) of weighted UniFrac distance (Fig. 5D) and analysis of similarity (ANOSIM) (Fig. 5E) also showed that the gut microbiota changed greatly in the colonic content after IMI treatment. At the phylum level, a higher abundance of *Bacteroidetes* but lower abundances of *Firmicutes*, *Cyanobacteria*, *Verrucomicrobia* and *TM7* were observed in the 30 mg/L

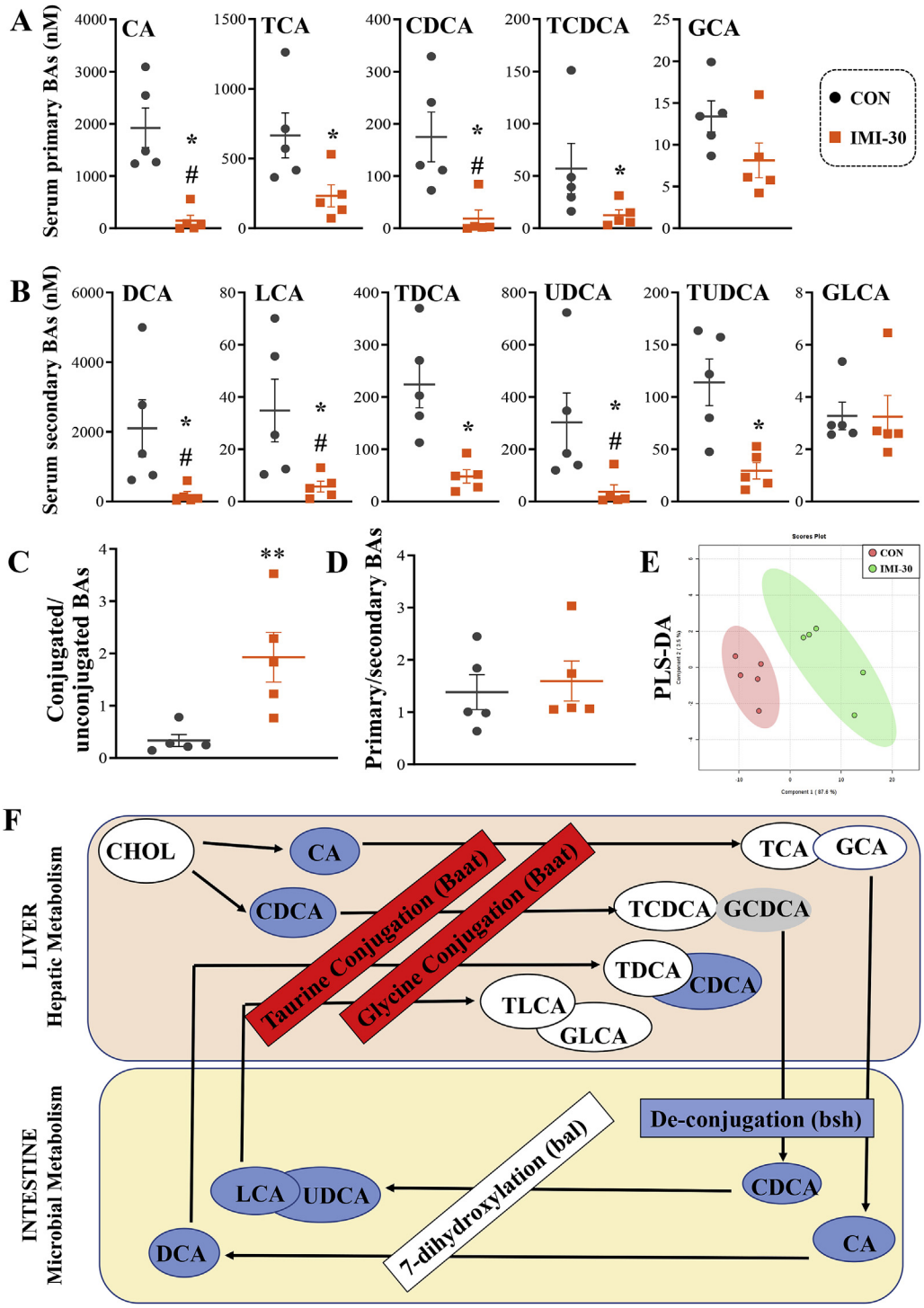


**Fig. 2.** Effects of IMI exposure on the BAs levels in the serum of mice. Different types of BA levels in the serum (A, B); ratio of conjugated/free BAs (C); ratio of primary/secondary BAs (D); OPLS-DA of serum BAs (E); effect of IMI on the hepatic and microbial metabolism of individual BA species in mice. Ovals represent BAs species, while rectangles represent genes involved in BAs metabolism. Boxes represent the location of the metabolic reaction and the source of the enzyme involved. Red represents 'increased levels', blue represents 'decreased levels', white represents 'no change', and gray represents 'not detected'. The color of each BA depicts the direction of change within the serum relative to that in the vehicle controls (F). The presented values are the means ± SEMs. *, $p < 0.05$, #, VIP value in OPLS-DA >1. (For interpretation of the references to color in this figure legend, the reader is referred to the Web version of this article.)

IMI-treated group (Fig. 5F). Interestingly, at the genus level, the abundance of *Akkermansia* increased significantly in the top ten most abundant species, and the abundance of *Allobaculum* decreased significantly in the IMI-treated group (Fig. 5G).

Furthermore, we also observed that in the IMI-treated group, the number of gram-negative bacteria increased, while the number of gram-positive bacteria decreased (Fig. 5H). In addition, the number of aerobic bacteria increased, and the number of anaerobic bacteria decreased in the IMI-exposed groups (Fig. 5I).

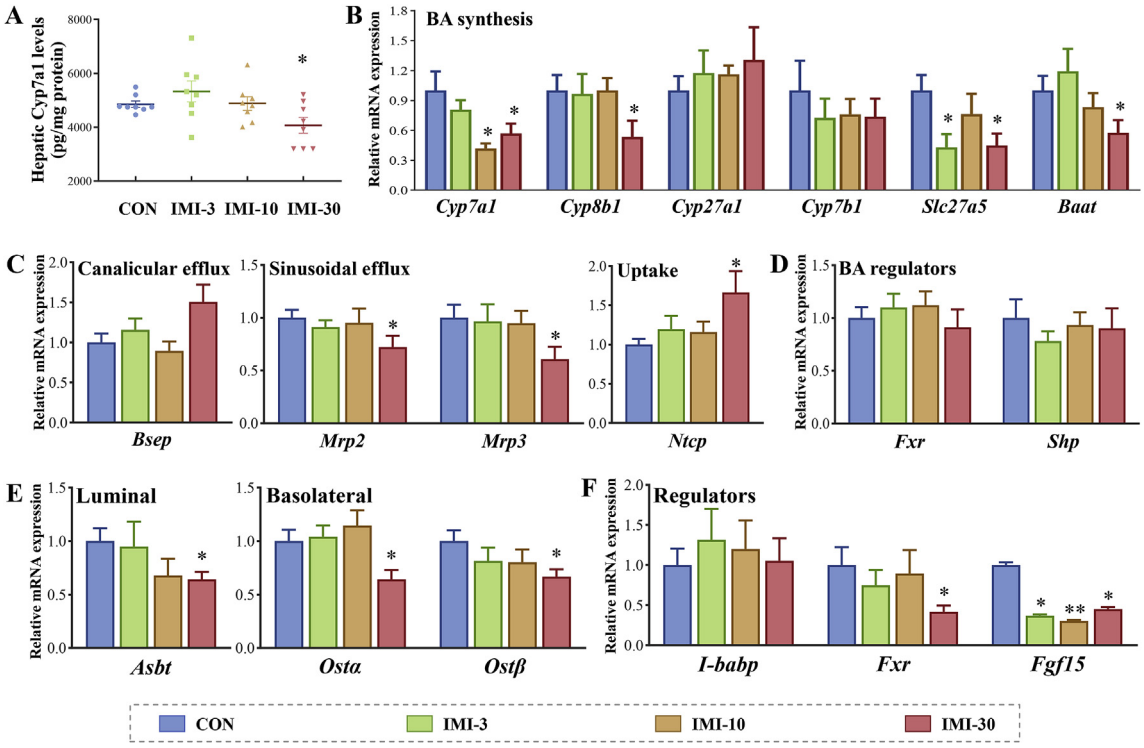


**Fig. 3.** Effects of IMI exposure on the transcription of genes related to BAs metabolism in the liver and ileum of mice. The hepatic Cyp7a1 levels in the liver (A); transcriptional status of genes involved in BAs synthesis in the liver (B); transcriptional status of genes involved in BAs transportation in the liver (C); transcriptional status of genes involved in BAs regulation of liver (D); transcriptional status of genes involved in BAs reabsorption in the ileum (E); transcriptional status of genes involved in BAs regulation in the ileum (F). All the data are expressed as the means ± SEMs. An asterisk indicates a significant difference (*at $p < 0.05$; **at $p < 0.01$) between the control and IMI-treated groups.

## 4. Discussion

In animals, the liver is a vital organ for metabolism and plays a role in deoxidation, storage of glycogen, synthesis of secreted proteins, and BA production in the body (Wahlström et al., 2016). Neonicotinoid insecticides have been found to cause oxidative stress in the liver and damage liver function in Institute of Cancer Research (ICR) mice (Yan et al., 2020). One survey founded that 45 mg $kg^{-1}$ bw $d^{-1}$ IMI induced dilations of central vein and sinusoids between hepatocytes, and the plasma levels of AST, ALT and AKP were significant increases in the treated female albino rats (Toor et al., 2013). Oral administration of IMI at 20 mg $kg^{-1}$ bw $d^{-1}$ for 90 days has generated oxidative stress and lipid peroxidation in liver of female Rats (Kapoor et al., 2010). Short time (2 h) after 10 μM IMI was administrated intravenously, the rats were founded to have oxidative stress and inflammation in central nervous system and liver (Duzguner and Erdogan, 2010). In the present study, 30 mg/L IMI exposure for 10 weeks decreased the relative liver weight of the male mice, caused histological damage, impaired liver function, and induced oxidative stress in the liver (Fig. 1). As previous evidence, liver injury could affect the synthesis of BAs (Wahlström et al., 2016; Ma et al., 2019). Thus, we thought the IMI induced liver damage might be a possible reason for BAs metabolism. What's more, treatment with 45 mg $kg^{-1}$ bw $d^{-1}$ IMI for 21 days increased serum cholesterol levels in adult rats (Hassan et al., 2019). Cholesterol can be catalyzed by a series of enzymes in the liver to produce BAs. In humans, primary BAs (CA and CDCA) are transported into the bile by the bile salt output pump (Bsep) after conjugated with glycine or taurine, and then stored in the gallbladder (Wahlström et al., 2016). After a meal, BAs are released into the gut to promote dietary lipid digestion. On the other hand, BAs control soluble vitamin uptake and provide an excretion mechanism for excessive hepatic cholesterol (Di Ciaula et al., 2017). Previous studies have found that p,p'-dichlorodiphenyldichloroethylene and β-hexachlorocyclohexane (a breakdown product of organochloride pesticides) (Liu et al., 2017) and the fungicide propamocarb (Wu et al., 2018b) cause BAs metabolism disorder, suggesting that BAs may be a potential target of pesticide toxicity. In addition, the synthesis, transport and regulation of BAs were also affected by IMI exposure.

In animals, low levels of BAs can cause malabsorption of lipids and fat-soluble vitamins in the gut (Vanderpas et al., 1987). The experimental results indicated that the serum and hepatic TBAs decreased (Fig. S1), which may have resulted from the decreased levels of the genes related to hepatic BA synthesis of IMI exposed mice (Fig. 2 A and B). Correspondingly, we found that the content of serum CA decreased after exposure to IMI (Fig. 2A), which is consistent with the decreased expression of hepatic Cyp8b1 (key enzyme necessary for CA production) (Fig. 3B) (Li and Chiang, 2014). At the same time, the rate-limiting enzyme Cyp7a1 in BAs synthesis also decreased (Fig. 3A and B), indicating a decrease in de novo hepatic BAs synthesis (Li et al., 2018). The synthesis of BAs in the pathways are all reduced after IMI treatment (Fig. 2F), which might affect lipid absorption and cholesterol metabolism. Some studies have unveiled new functions of BAs as signaling molecules and metabolic integrators (Chiang, 2013; Chávez-Talavera et al., 2017). Fxr, related to the body's metabolic diseases, can be activated by BAs in the terminal ileum (Lickteig et al., 2016). Treating bile duct ligation (BDL) mice with probiotic Lactobacillus rhamnosus GG (LGG) can decrease hepatic BAs levels by increasing the intestinal Fxr/Fgf15 signaling pathway-mediated suppression of de novo BAs synthesis and enhance BAs excretion (Liu et al., 2019). In contrast, the mRNA levels of ileal Fxr and Fgf 15 decreased in the IMI-exposed mice (Fig. 3F), and we speculated that there might be a

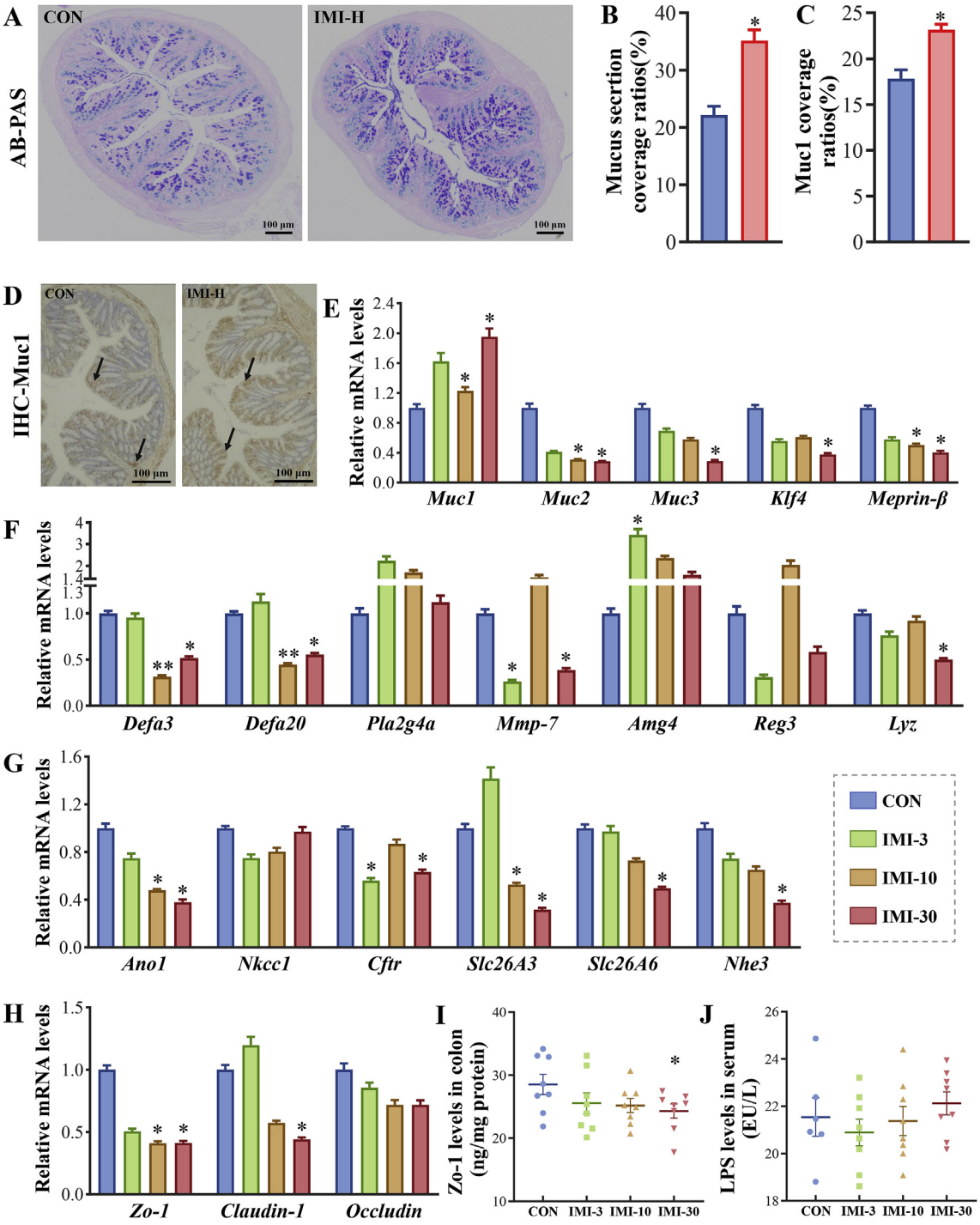


**Fig. 4.** Effects of IMI exposure on the gut barrier in the colon of mice. AB-PAS staining and the ratio of the mucus secretion area to the entire colon area (A, B); colonic immunohistochemical staining and normalized colonic Muc1 secretion. Black arrow indicates Muc1 protein (C, D); the relative mRNA levels of genes related to the secretion of mucus in the colon (E); the relative mRNA levels of AMPs in the colon (F); the relative mRNA levels of ion transport-related genes in the colon (G); the relative mRNA levels of tight junction-associated genes in the colon (H); the protein levels of colonic Zo-1 (I); the serum LPS levels (J). All the data are expressed as the means±SEMs. An asterisk indicates a significant difference (*at $p < 0.05$; **at $p < 0.01$) between the control and IMI-treated groups.

compensation adjustment of the low hepatic BA levels to maintain a constant level of BAs. At the terminal ileum, most (90%–95%) BAs are reabsorbed via the apical membrane sodium-dependent bile salt transporter (Asbt) (Out et al., 2015; Wahlström et al., 2016; Xiao and Pan, 2017). Therefore, the decreased expression of ileal Asbt will cause a decrease in the amount of BAs reabsorbed by the liver and an increase in the amount of BAs excreted by feces, which may lead to disorders of BA pools (Dawson et al., 2003). This experiment found that the mRNA level of *Asbt* in the ileum was reduced (Fig. 3E), indicating that IMI might reduce the reabsorption of BAs in the ileum. This result may explain the decrease in BA levels in the liver and serum and the increase in fecal BA levels (Fig. S1). Lack of BAs in the gut could lead to the destruction of the colonic barrier, imbalance of the gut microbiota and excess growth of gram-

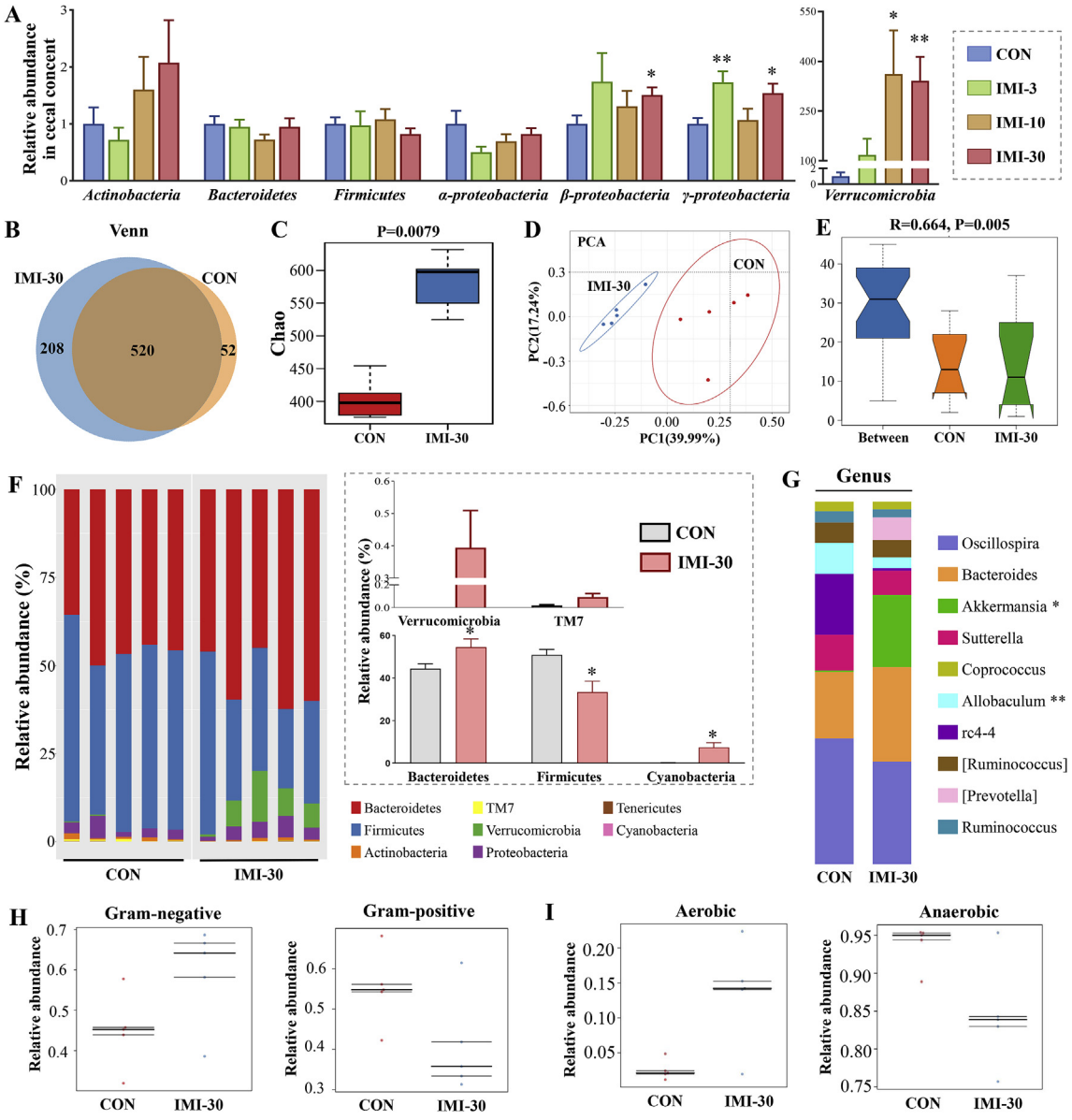


**Fig. 5.** IMI exposure induced colonic microbiota dysbiosis in mice. The variation in the cecal microbiota at the phylum level (A); the OTUs of bacteria in the colonic contents after IMI exposure (B); the Chao index of α-diversity in the colonic microbiota (C); weighted UniFrac distance PCoA estimates and analysis of similarity (ANOSIM) of the colonic microbiota (D, E); the relative abundances of microbiota constituents in the colon detected by 16S RNA gene sequencing (F); the top 10 core genera of the colonic microbiota (G). Relative content of gram-negative and gram-positive bacteria in colonic contents (H). Relative content of anaerobic and aerobic bacteria in colon contents (I). All the data are expressed as the means ± SEMs. An asterisk indicates a significant difference (*at $p < 0.05$; **at $p < 0.01$) between the control and IMI-treated groups.

negative bacteria. Moreover, sequencing of the colonic contents revealed that the α-diversity and OTUs of the intestinal flora increased, and the gut microbiota lost balance with the overgrowth of gram-negative bacteria in IMI exposed mice (Fig. 5B, C and 5H).

The gut microbiota can affect the BA composition, hydrophobicity and pool size (Jin et al., 2017; Wang et al., 2019). In the intestine, primary BAs are uncoupled by the microbial community and converted into secondary BAs, which consist mainly of DCA and LCA (Wahlström et al., 2016). Antibiotic treatment of Wistar rats caused significant changes in primary and secondary bile acids, causing an imbalance in the BA metabolism pool (Behr et al., 2019). In the intestine, conjugated BAs are hydrolyzed into their free form by bacterial enzymes, known as BSH (Zhou et al., 2018). Exposure of mice to organochlorine pesticides increases the amounts of lactobacilli with bile salt hydrolase (BSH) activity, and the BAs in the gallbladder become more hydrophobic (Liu et al., 2017). In this experiment, it was found that the abundance of Firmicutes decreased and that of Bacteroidetes increased (Fig. 5F), which might weaken the deconjugation of BAs (Bustos et al., 2018; Song et al., 2019), and the deconjugated BAs are more hydrophobic and easier to excrete into the feces. In addition, low ratio of Firmicutes/Bacteroidetes may affect the absorption of nutrients and then reduce relative liver weight (Indiani et al., 2018). Because fecal deconjugated BAs content is reduced, it is presumed that the reabsorption of deconjugated BAs is reduced (Fig. 2C). Some microorganisms (mainly anaerobic bacteria) with 7α-dehydroxyl activity can change the primary BAs into secondary BAs (Ridlon et al., 2006), but this activity was decreased in this experiment (Fig. 5I); however, the ratio of primary/secondary BAs was not affected (Fig. 2D). The abundance of Akkermansia, a genus of mucus-

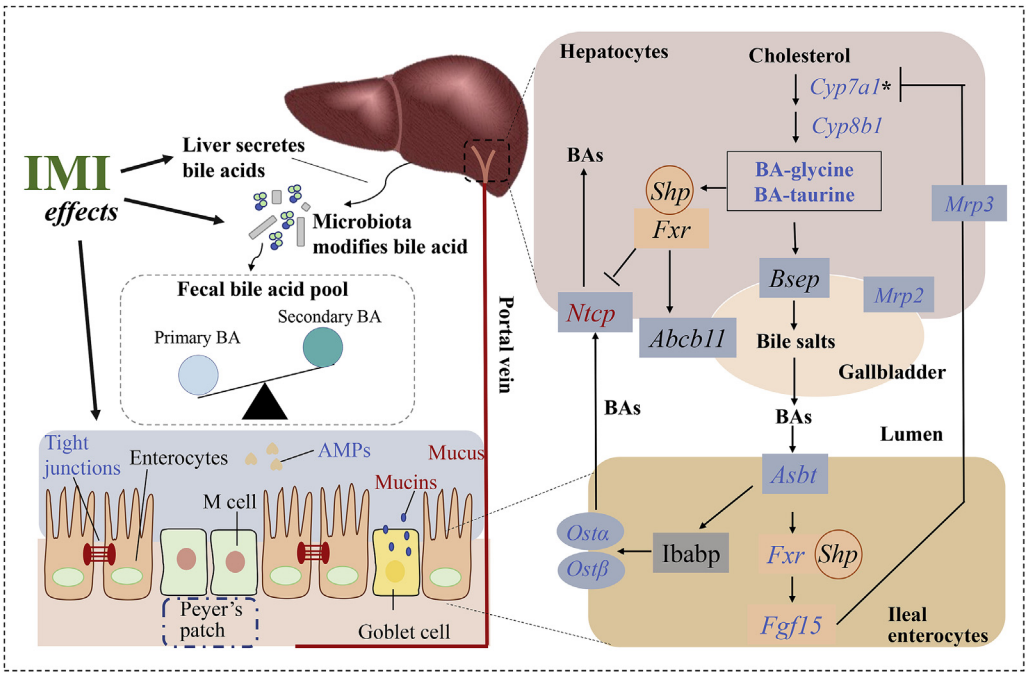


**Fig. 6.** Schematic diagram of the mechanism by which IMI affects BA metabolism by disrupting the colonic barrier, regulating the gut microbiota, reducing ileal BAs intake, and reducing liver BAs synthesis. Red represents 'increased levels', blue represents 'decreased levels', and black represents 'no change' or 'untested'. The color of each gene or factor depicts the direction of change relative to vehicle controls in mice. (For interpretation of the references to color in this figure legend, the reader is referred to the Web version of this article.)

degrading bacteria (Li et al., 2019), increased in this experiment (Fig. 5G). We studied the intestinal barrier and found that the mucus content increased greatly, overexpression of Muc-1 in the colon epithelium (Fig. 4C and D) could aggravates colonic inflammation (Kadayakkara et al., 2010; Cascio et al., 2017). That meant that gut barrier was damaged, so the body was more vulnerable to pesticide poisoning.

Intestinal BAs can inhibit the proliferation and translocation of the intestinal flora and have a certain effect on maintaining the stability of intestinal barrier function (Ikegami and Honda, 2018; Hofmann and Eckmann, 2006). Our experimental results show that the BA levels in the liver and serum decrease (Fig. S1); therefore, the content of BAs released from the gallbladder into the small intestine decreases. In addition, the expression of colonic tight junction-associated proteins decreased, and the secretion of mucus largely increased (Fig. 4). The gut barrier function was greatly impaired by IMI exposure, which might increase the body's susceptibility to harmful substances in the gut. Intestinal BAs can act as a chemical barrier for the intestinal mucosa and remove LPS (Liang et al., 2019). The increase in gram-negative bacterial levels in the gut and the destruction of the intestinal barrier will increase the probability of LPS entering the blood (Liang et al., 2019). LPS binds to ligands of many tissues and therefore induces a series of diseases, such as liver inflammation, neuroinflammation, and insulin resistance (Benoit et al., 2015; Suez et al., 2014; Org et al., 2017). The results of this experiment showed that serum LPS content had an upward trend, but this trend was not statistically significant (Fig. 4J).

In conclusion, to our knowledge, for the first time, we showed the mechanism by which low-dose IMI exposure damaged liver function and the intestinal barrier and disrupted the homeostasis of BAs and the gut microbiota. The meachanism was showed in Fig. 6. These effects occurred through (I) inhibiting de novo synthesis of hepatic BAs; (II) reducing ileal BA reabsorption; (III) destroying the colonic intestinal barriers; and (IV) influencing the structure and composition of gut microbiota, which is related to the BA pool. Taken together, some parameters could be affected by the pesticide even the exposure concentrations were very lower, indicating that the risk of some pesticide was underestimated. We hoped that much more studies could be performed to evaluate the toxicity of pesticides from some new perspectives.

## Credit author statement

Guiling Yang: Conceptualization, Writing- Original draft preparation; Xianling Yuan: Methodology, Writing; Cuiyuan Jin: Validation, Investigation; Dou Wang: Validation, Investigation; Yanhua Wang: Supervision, Writing- Reviewing and Editing; Wenyu Miao: Data curation; Yuanxiang Jin: Supervision, Writing- Reviewing and Editing.

## Declaration of competing interest

The authors declare that they have no known competing financial interests or personal relationships that could have appeared to influence the work reported in this paper.

## Acknowledgments

The research was supported by the National Key Research and Development Program of China (Grant No. 2018YFC1603004), State Key Laboratory for Managing Biotic and Chemical Threats to the Quality and Safety of Agro-products (2010DS700124-KF2002) and Zhejiang Provincial Natural Science Foundation of China (LR16B070002).

## Appendix A. Supplementary data

Supplementary data to this article can be found online at https://doi.org/10.1016/j.envpol.2020.115290.

## References


Arfat, Y., Mahmood, N., Tahir, M.U., Rashid, M., Anjum, S., Zhao, F., et al., 2014. Effect of imidacloprid on hepatotoxicity and nephrotoxicity in male albino mice. Toxicol. Rep. 1, 554–561.

Banerjee, B.D., 1999. The influence of various factors on immune toxicity assessment of pesticide chemicals. Toxicol. Lett. 107, 21–31.

Batikian, C.M., Lu, A., Watanabe, K., Pitt, J., Gersberg, R.M., 2019. Temporal pattern in levels of the neonicotinoid insecticide, imidacloprid, in an urban stream. Chemosphere 223, 83–90.

Behr, C., Slopianka, M., Haake, V., Strauss, V., Sperber, S., Kamp, H., et al., 2019. Analysis of metabolome changes in the bile acid pool in feces and plasma of antibiotic-treated rats. Toxicol. Appl. Pharmacol. 363, 79–87.

Benoit, C., Omry, K., Julia, G., Angela, P., Shanthi, S., Ley, R.E., et al., 2015. Dietary emulsifiers impact the mouse gut microbiota promoting colitis and metabolic syndrome. Nature 519, 92–96.

Brunet, J.L., Maresca, M., Fantini, J., Belzunces, L.P., 2004. Human intestinal absorption of imidacloprid with Caco-2 cells as enterocyte model. Toxicol. Appl. Pharmacol. 194, 1–9.

Bustos, A.Y., Font de Valdez, G., Fadda, S., Taranto, M.P., 2018. New insights into bacterial bile resistance mechanisms: the role of bile salt hydrolase and its impact on human health. Food Res. Int. 112, 250–262.

Cascio, S., Faylo, J.L., Sciurba, J.C., Xue, J., Ranganathan, S., Lohmueller, J.J., et al., 2017. Abnormally glycosylated MUC1 establishes a positive feedback circuit of inflammatory cytokines, mediated by NF-κB p65 and EzH2, in colitis-associated cancer. Oncotarget 8, 105284–105298.

Chávez-Talavera, O., Tailleux, A., Lefebvre, P., Staels, B., 2017. Bile acid control of metabolism and inflammation in obesity, type 2 diabetes, dyslipidemia, and nonalcoholic fatty liver disease. Gastroenterology 152, 1679–1694.

Chen, D.W., Zhang, Y.P., Lv, B., Liu, Z.B., Han, J.G., Li, J.G., et al., 2019. Dietary exposure to neonicotinoid insecticides and health risks in the Chinese general population through two consecutive total diet studies. Environ. Int. 135, 105399–105412.

Chiang, J.Y., 2013. Bile acid metabolism and signaling. Comp. Physiol. 3, 1191–1212.

Csanaky, I.L., Lickteig, A.J., Klaassen, C.D., 2018. Aryl hydrocarbon receptor (AhR) mediated short-term effects of 2,3,7,8-tetrachlorodibenzo-p-dioxin (TCDD) on bile acid homeostasis in mice. Toxicol. Appl. Pharmacol. 343, 48–61.

Daisley, B.A., Trinder, M., McDowell, T.W., Welle, H., Dube, J.S., Ali, S.N., et al., 2017. Neonicotinoid-induced pathogen susceptibility is mitigated by Lactobacillus plantarum immune stimulation in a Drosophila melanogaster model. Sci. Rep. 7, 2703–2716.

Damalas, C.A., Eleftherohorinos, I.G., 2011. Pesticide exposure, safety issues, and risk assessment indicators. Int. J. Environ. Res. Publ. Health 8, 1402–1419.

Dawson, P.A., Haywood, J., Craddock, A.L., Wilson, M., Tietjen, M., Kluckman, K., et al., 2003. Targeted deletion of the ileal bile acid transporter eliminates enterohepatic cycling of bile acids in mice. J. Biol. Chem. 278, 33920–33927.

Di Ciaula, A., Garruti, G., Lunardi Baccetto, R., Molina-Molina, E., Bonfrate, L., Wang, D.Q., et al., 2017. Bile acid physiology. Ann. Hepatol. 16, 4–14.

Dupont, A., Heinbockel, L., Brandenburg, K., Hornef, M.W., 2014. Antimicrobial peptides and the enteric mucus layer act in concert to protect the intestinal mucosa. Gut Microb. 5, 761–765.

Duzguner, V., Erdogan, S., 2010. Acute oxidant and inflammatory effects of imidacloprid on the mammalian central nervous system and liver in rats. Pestic. Biochem. Physiol. 97, 13–18.

Fader, K.A., Nault, R., Zhang, C., Kumagai, K., Harkema, J.R., Zacharewski, T.R., 2017. 2,3,7,8-Tetrachlorodibenzo-p-dioxin (TCDD)-elicited effects on bile acid homeostasis: alterations in biosynthesis, enterohepatic circulation, and microbial metabolism. Sci. Rep. 7, 5921–5938.

Ferrell, J.M., Chiang, J.Y.L., 2019. Understanding bile acid signaling in diabetes: from pathophysiology to therapeutic targets. Diabetes Metab. J 43, 257–272.

Hassan, A.M.S., Abo El-Ela, F.I., Abdel-Aziz, A.M., 2019. Investigating the potential protective effects of natural product quercetin against imidacloprid-induced biochemical toxicity and DNA damage in adults rats. Toxicol. Rep. 6, 727–735.

Hofmann, A.F., Eckmann, L., 2006. How bile acids confer gut mucosal protection against bacteria. Proc. Natl. Acad. Sci. U. S. A. 103, 333–334.

Ikegami, T., Honda, A., 2018. Reciprocal interactions between bile acids and gut microbiota in human liver diseases. Hepatol. Res. 48, 15–27.

Indiani, C.M.D.S.P., Rizzardi, K.F., Castelo, P.M., Ferraz, L.F.C., Darrieux, M., Parisotto, T.M., 2018. Childhood obesity and firmicutes/bacteroidetes ratio in the gut microbiota: a systematic review. Child. Obes. 14, 501–509.

Jin, C.Y., Luo, T., Fu, Z.W., Jin, Y.X., 2018a. Chronic exposure of mice to low doses of imazalil induces hepatotoxicity at the physiological, biochemical, and transcriptomic levels. Environ. Toxicol. 33, 650–658.

Jin, C.Y., Xia, J.Z., Wu, S.S., Tu, W.Q., Pan, Z.H., Fu, Z.W., et al., 2018b. Insights into a possible influence on gut microbiota and intestinal barrier function during chronic exposure of mice to imazalil. Toxicol. Sci. 162, 113–123.

Jin, C.Y., Zhang, R., Fu, Z.W., Jin, Y.X., 2019a. Maternal exposure to imazalil disrupts the endocrine system in F1 generation mice. Mol. Cell. Endocrinol. 486, 105–112.

Jin, Y.X., Lu, L., Tu, W.Q., Luo, T., Fu, Z.W., 2019b. Impacts of polystyrene microplastic on the gut barrier, microbiota and metabolism of mice. Sci. Total Environ. 649, 308–317.

Jin, Y.X., Wu, S.S., Zeng, Z.Y., Fu, Z.W., 2017. Effects of environmental pollutants on gut microbiota. Environ. Pollut. 222, 1–9.

Kapoor, U., Srivastava, M.K., Bhardwaj, S., Srivastava, L.P., 2010. Effect of imidacloprid on antioxidant enzymes and lipid peroxidation in female rats to derive its No Observed Effect Level (NOEL). J. Toxicol. Sci. 35, 577–581.

Kadayakkara, D.K., Beatty, P.L., Turner, M.S., Janjic, J.M., Ahrens, E.T., Finn, O.J., 2010. Inflammation driven by overexpression of the hypoglycosylated abnormal Mucin 1 (MUC1) links inflammatory bowel disease and pancreatitis. Pancreas 39, 510–515.

Liang, Y.R., Zhan, J., Liu, D.H., Luo, M., Han, J.J., Liu, X.K., et al., 2019. Organophosphorus pesticide chlorpyrifos intake promotes obesity and insulin resistance through impacting gut and gut microbiota. Microbiome 7, 19–34.

Lickteig, A.J., Csanaky, I.L., Pratt-Hyatt, M., Klaassen, C.D., 2016. Activation of constitutive androstane receptor (CAR) in mice results in maintained biliary excretion of bile acids despite a marked decrease of bile acids in liver. Toxicol. Sci. 151, 403–418.

Li, C.Y., Dempsey, J.L., Wang, D., Lee, S., Weigel, K.M., Fei, Q., et al., 2018. PBDEs altered gut microbiome and bile acid homeostasis in male C57BL/6 mice. Drug Metab. Dispos. 46, 1226–1240.

Li, T., Chiang, J.Y., 2014. Bile acid signaling in metabolic disease and drug therapy. Pharmacol. Rev. 66, 948–983.

Liu, Q., Shao, W.T., Zhang, C.L., Xu, C., Wang, Q.H., Liu, H., et al., 2017. Organochloride pesticides modulated gut microbiota and influenced bile acid metabolism in mice. Environ. Pollut. 226, 268–276.

Li, X., Brejnrod, A.D., Ernst, M., Rykær, M., Herschend, J., Olsen, N.M.C., et al., 2019. Heavy metal exposure causes changes in the metabolic health-associated gut microbiome and metabolites. Environ. Int. 126, 454–467.

Liu, Y., Chen, K., Li, F., Gu, Z., Liu, Q., He, L., et al., 2019. Probiotic lactobacillus rhamnosus GG prevents liver fibrosis through inhibiting hepatic bile acid synthesis and enhancing bile acid excretion in mice. Hepatology. https://doi.org/10.1002/hep.30975.

Luo, T., Shen, M.L., Zhou, J.J., Wang, X.Y., Xia, J.Z., Fu, Z.W., et al., 2019. Chronic exposure to low doses of Pb induces hepatotoxicity at the physiological, biochemical, and transcriptomic levels of mice. Environ. Toxicol. 34, 521–529.

Ma, Z., Wang, X., Yin, P., Wu, R., Zhou, L., Xu, G., et al., 2019. Serum metabolome and targeted bile acid profiling reveals potential novel biomarkers for drug-induced liver injury. Medicine (Baltim.) 98, e16717.

Mukherjee, S., Hooper, L.V., 2015. Antimicrobial defense of the intestine. Immunity 42, 28–39.

Mu, Q., Kirby, J., Reilly, C.M., Luo, X.M., 2017. Leaky gut as a danger signal for autoimmune diseases. Front. Immunol. 8, 598–608.

Org, E., Blum, Y., Kasela, S., Mehrabian, M., Kuusisto, J., Kangas, A.J., et al., 2017. Relationships between gut microbiota, plasma metabolites, and metabolic syndrome traits in the METSIM cohort. Genome Biol. 18, 70.

Out, C., Patankar, J.V., Doktorova, M., Boesjes, M., Bos, T., de Boer, S., et al., 2015. Gut microbiota inhibit Asbt-dependent intestinal bile acid reabsorption via Gata4. J. Hepatol. 63, 697–704.

Pan, Z.H., Yuan, X.L., Tu, W.Q., Fu, Z.W., Jin, Y.X., 2019. Subchronic exposure of environmentally relevant concentrations of F-53B in mice resulted in gut barrier dysfunction and colonic inflammation in a sex-independent manner. Environ. Pollut. 253, 268–277.

Ridlon, J.M., Kang, D.J., Hylemon, P.B., 2006. Bile salt biotransformations by human intestinal bacteria. J. Lipid Res. 47, 241–259.

Rizzetto, L., Fava, F., Tuohy, K.M., Selmi, C., 2018. Connecting the immune system, systemic chronic inflammation and the gut microbiome: the role of sex. J. Autoimmun. 92, 12–34.

Sheng, N., Pan, Y., Guo, Y., Sun, Y., Dai, J., 2018. Hepatotoxic effects of hexafluoropropylene oxide trimer acid (HFPO-TA), A novel perfluorooctanoic acid (PFOA) alternative, on mice. Environ. Sci. Technol. 52, 8005–8015.

Song, Z., Cai, Y., Lao, X., Wang, X., Lin, X., Cui, Y., et al., 2019. Taxonomic profiling and populational patterns of bacterial bile salt hydrolase (BSH) genes based on worldwide human gut microbiome. Microbiome 7, 9.

Sriapha, C., Trakulsrichai, S., Intaraprasong, P., Wongvisawakorn, S., Tongpoo, A., Schimmel, J., et al., 2020. Imidacloprid poisoning case series: potential for liver injury. Clin. Toxicol. 58, 136–138.

Suez, J., Korem, T., Zeevi, D., Zilberman-Schapira, G., Thaiss, C.A., Maza, O., et al., 2014. Artificial sweeteners induce glucose intolerance by altering the gut microbiota. Nature 514, 181–186.

Sun, Q.C., Xiao, X., Kim, Y., Kim, D., Yoon, K.S., Clark, J.M., et al., 2016. Imidacloprid promotes high fat diet-induced adiposity and insulin resistance in male C57BL/6J Mice. J. Agric. Food Chem. 64, 9293–9306.

Toor, H.K., Sangha, G.K., Khera, K.S., 2013. Imidacloprid induced histological and biochemical alterations in liver of female albino rats. Pestic. Biochem. Physiol. 105, 1–4.

Vanderpas, J.B., Koopman, B.J., Cadranel, S., Vandenbergen, C., Rickaert, F., Quenon, M., et al., 1987. Malabsorption of liposoluble vitamins in a child with bile acid deficiency. J. Pediatr. Gastroenterol. Nutr. 6, 33–41.

Wahlström, A., Sayin, S.I., Marschall, H.U., Bäckhed, F., 2016. Intestinal crosstalk between bile acids and microbiota and its impact on host metabolism. Cell Metabol. 24, 41–50.

Wang, D.Z., Yan, S., Yan, J., Teng, M.M., Meng, Z.Y., Li, R.S., et al., 2019. Effects of triphenyl phosphate exposure during fetal development on obesity and

metabolic dysfunctions in adult mice: impaired lipid metabolism and intestinal dysbiosis. Environ. Pollut. 246, 630–638.
Wei, T., Tian, W.L., Liu, F.N., Xie, G.H., 2014. Protective effects of exogenous β-hydroxybutyrate on paraquat toxicity in rat kidney. Biochem. Biophys. Res. Commun. 447, 666–671.
Wu, S.S., Jin, C.Y., Wang, Y.Y., Fu, Z.W., Jin, Y.X., 2018a. Exposure to the fungicide propamocarb causes gut microbiota dysbiosis and metabolic disorder in mice. Environ. Pollut. 237, 775–783.
Wu, S.S., Luo, T., Wang, S.Y., Zhou, J.C., Ni, Y.C., Fu, Z.W., et al., 2018b. Chronic exposure to fungicide propamocarb induces bile acid metabolic disorder and increases trimethylamine in C57BL/6J mice. Sci. Total Environ. 642, 341–348.
Xia, J.Z., Jin, C.Y., Pan, Z.H., Sun, L.W., Fu, Z.W., Jin, Y.X., 2018. Chronic exposure to low concentrations of lead induces metabolic disorder and dysbiosis of the gut microbiota in mice. Sci. Total Environ. 631–632, 439–448.
Xiao, L., Pan, G., 2017. An important intestinal transporter that regulates the enterohepatic circulation of bile acids and cholesterol homeostasis: the apical sodium-dependent bile acid transporter (SLC10A2/ASBT). Clin. Res. Hepatol. Gastroenterol. 41, 509–515.
Yan, S., Meng, Z.Y., Tian, S.N., Teng, M.M., Yan, J., Jia, M., et al., 2020. Neonicotinoid insecticides exposure cause amino acid metabolism disorders, lipid accumulation and oxidative stress in ICR mice. Chemosphere 246, 125661–125671.
Yuan, X.L., Pan, Z.H., Jin, C.Y., Ni, Y.H., Fu, Z.W., Jin, Y.X., 2019. Gut microbiota: an underestimated and unintended recipient for pesticide-induced toxicity. Chemosphere 227, 425–434.
Yuan, X.L., Shen, J.Y., Zhang, X.Y., Tu, W.Q., Fu, Z.W., Jin, Y.X., 2020. Imidacloprid disrupts the endocrine system by interacting with androgen receptor in male mice. Sci. Total Environ. 708, 135163.
Zhang, Q., Lu, Z.B., Chang, C.H., Yu, C., Wang, X.M., Lu, C.S., 2019b. Dietary risk of neonicotinoid insecticides through fruit and vegetable consumption in school-age children. Environ. Int. 126, 672–681.
Zhang, Y., Jin, C.Y., Wang, X.Y., Shen, M.L., Zhou, J.J., Wu, S.S., et al., 2019a. Propamocarb exposure decreases the secretion of neurotransmitters and causes behavioral impairments in mice. Environ. Toxicol. 34, 22–29.
Zhou, J., Tang, L., Wang, J., Wang, J.S., 2018. Aflatoxin B1 disrupts gut-microbial metabolisms of short-chain fatty acids, long-chain fatty acids, and bile acids in male F344 rats. Toxicol. Sci. 164, 453–464.